

Supplementary Materials: Defining Wildfire Susceptibility Maps in Italy for Understanding Seasonal Wildfire Regimes at National Level

Andrea Trucchia^{1*}, Giorgio Meschi¹, Paolo Fiorucci¹, Andrea Gollini², Dario Negro²

1. Corine 2018 Land Cover legend and distribution

Table S1. CLC Codes and their description. The class evidenced by the (*) symbol have not been used as input data of the machine learning model. For technical purposes, they have been merged into an *ad hoc* class "0".

CLC_CODE	Label
111	Continuous urban fabric (*)
112	Discontinuous urban fabric (*)
121	Industrial or commercial units (*)
122	Road and rail networks and associated land (*)
123	Port areas (*)
124	Airports (*)
131	Mineral extraction sites (*)
132	Dump sites (*)
133	Construction sites (*)
141	Green urban areas (*)
142	Sport and leisure facilities (*)
211	Non-irrigated arable land
212	Permanently irrigated land
213	Rice fields
221	Vineyards
222	Fruit trees and berry plantations
223	Olive groves
224	Other Permanent crops
231	Pastures
241	Annual crops associated with permanent crops
242	Complex cultivation patterns
243	Land principally occupied by agric., with significant areas of nat. veg.
244	Agro-forestry areas
311	Broad-leaved forest
312	Coniferous forest
313	Mixed forest
321	Natural grasslands
322	Moors and heathland
323	Sclerophyllous vegetation
324	Transitional woodland-shrub
331	Beaches, dunes, sands
332	Bare rocks
333	Sparsely vegetated areas
334	Burnt areas
335	Glaciers and perpetual snow
411	Inland marshes (*)
412	Peat bogs (*)
421	Salt marshes (*)
422	Salines (*)
423	Intertidal flats (*)
511	Water courses (*)
512	Water bodies (*)
521	Coastal lagoons (*)
522	Estuaries (*)
523	Sea and ocean (*)

2. Importance ranking of the neighboring vegetation variable

In the following, the importance ranking assessed by the ML algorithm (through the Gini Impurity method) is shown, for several groups of variables:

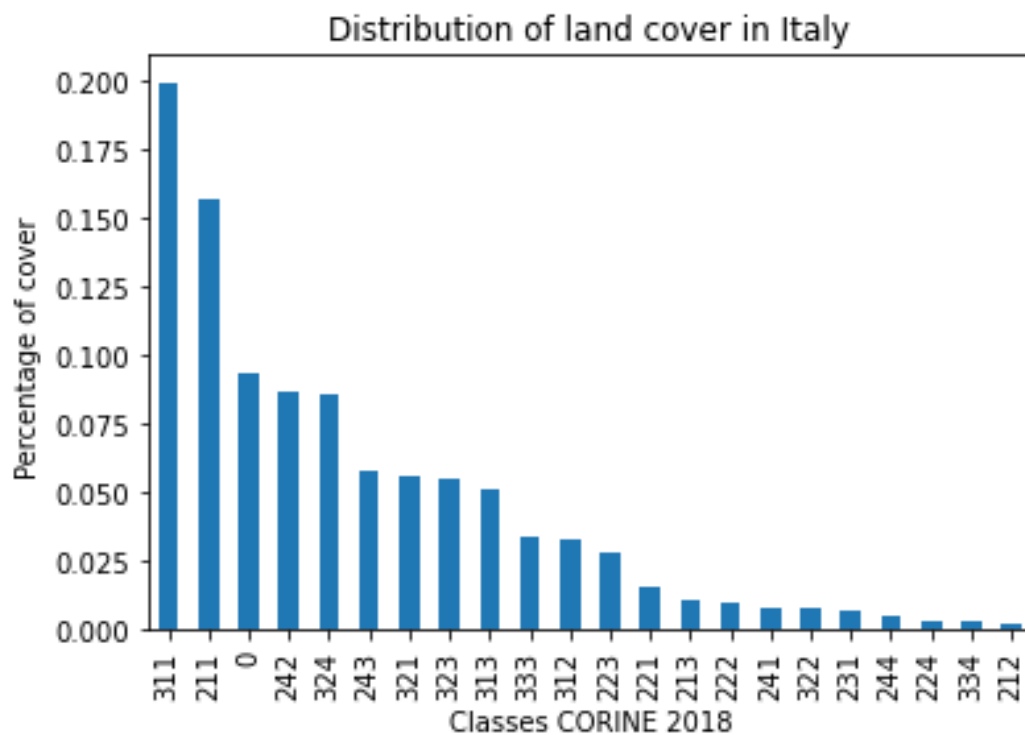


Figure S1. Distribution of the CORINE 2018 land cover classes in Italy, the class 0 refers to an aggregation of not burnable areas as specified in [S1](#)

- The variables that have been merged in the main Manuscript in the variable "neighbouring vegetation", are here represented in detail, in order to assess the importance of vegetation continuity for each vegetation/land use class of CLC18. This has been shown of course for both Summer and Winter wildfire seasons, in Figures [S2](#), [S3](#)
- The variables that have been merged in the main Manuscript in the variable "vegetation", corresponding to the vegetation of the analysed pixel are here represented in detail, in order to assess the impact of vegetation types for each vegetation/land use class of CLC18. Also this has been shown for both Summer and Winter wildfire seasons, see Figures [S4](#), [S5](#)

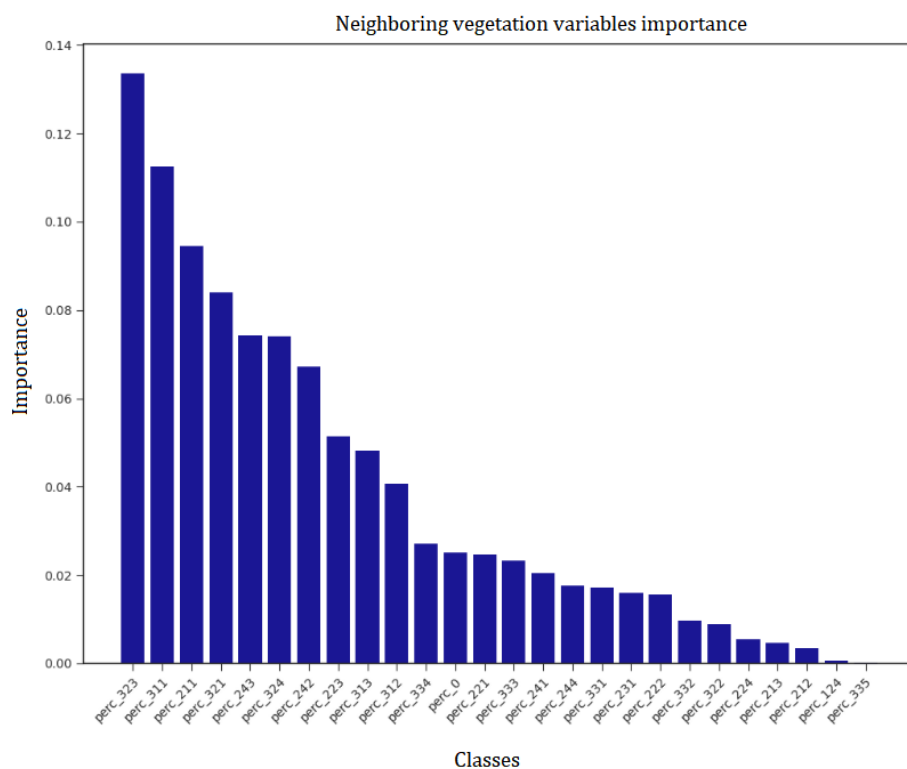


Figure S2. Importance ranking (Mean Decrease in Impurity) of the neighboring vegetation variable related to the summer’s seasonal analysis

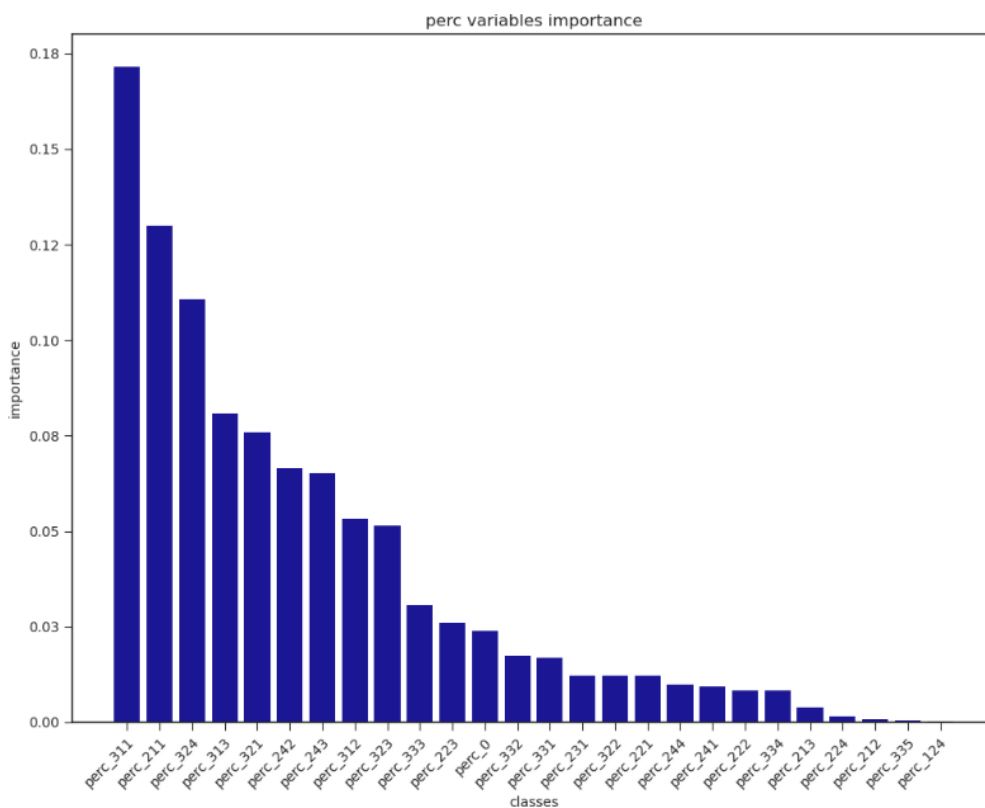


Figure S3. Importance ranking (Mean Decrease in Impurity) of the neighboring vegetation variable related to the winter’s seasonal analysis

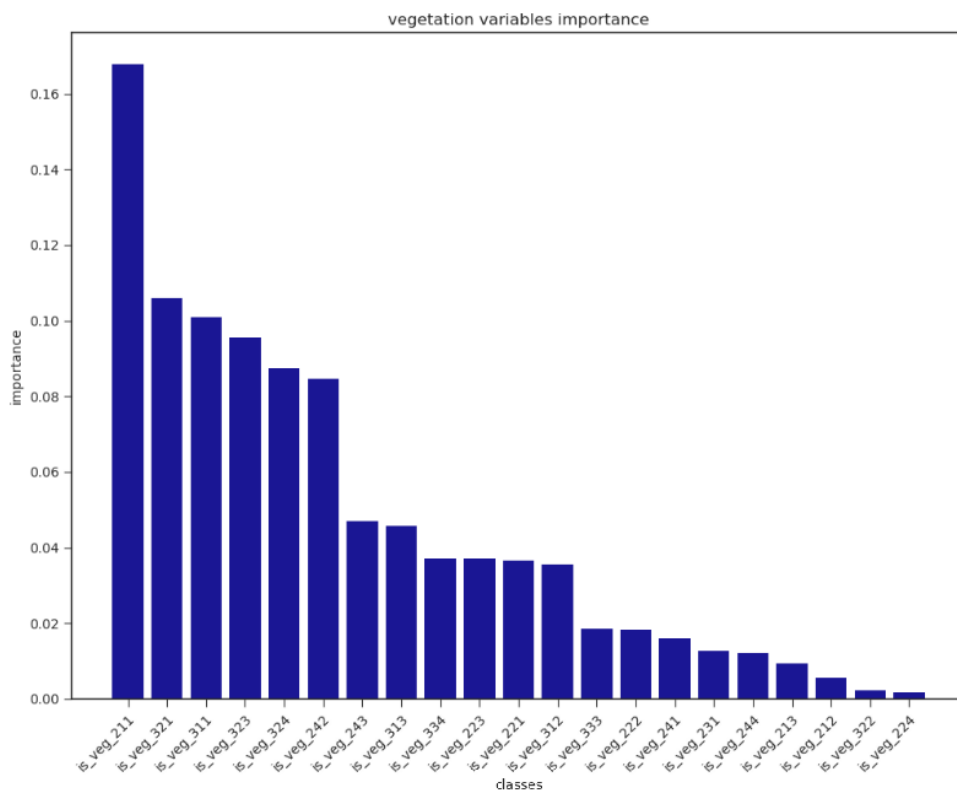


Figure S4. Importance ranking (Mean Decrease in Impurity) of the vegetation variable related to the summer’s seasonal analysis

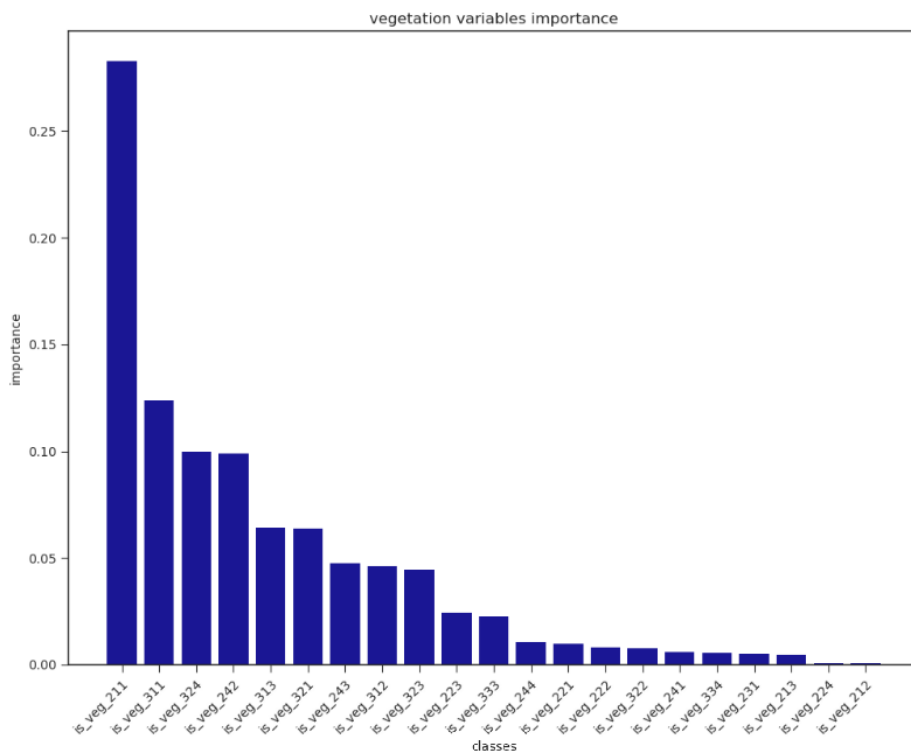


Figure S5. Importance ranking (Mean Decrease in Impurity) of the neighboring vegetation variable related to the winter’s seasonal analysis

3. Importance ranking of the neighboring vegetation variable

In the following, the four most important vegetation classes in the ranking of the previous Section are examined in detail, from both summer (CLC codes 211, 321, 311, 323) and winter (CLC codes 211, 311, 324, 242). Every pixel of the susceptibility map corresponding to the latter CLC codes has been retrieved and their susceptibility distribution has been plotted.

This highlighted different behaviours of those important classes: some classes are important to the ML algorithm because they are immediately associated with low susceptibility, such as arable land (211) and rice fields (242), while others are important because they are strongly associated with high susceptibility output (such as Sclerophyllous vegetation, 323). Other classes exhibit more complex behaviour, such as broad-leaves (311) and natural grassland (321). In this case, the interactions with other predisposing factors, such as DEM, slope and climate, is needed by the ML algorithm in order to assign a susceptibility value to the pixels characterized by such vegetation types.

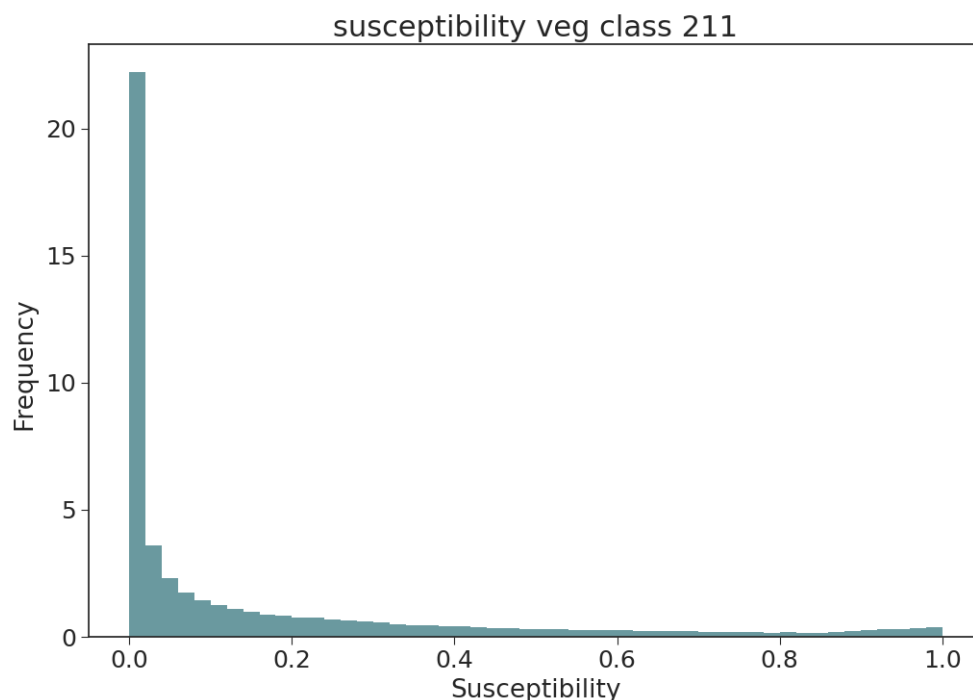


Figure S6. Normalized susceptibility distribution inside the non-irrigated arable land in the summer season (class 211).

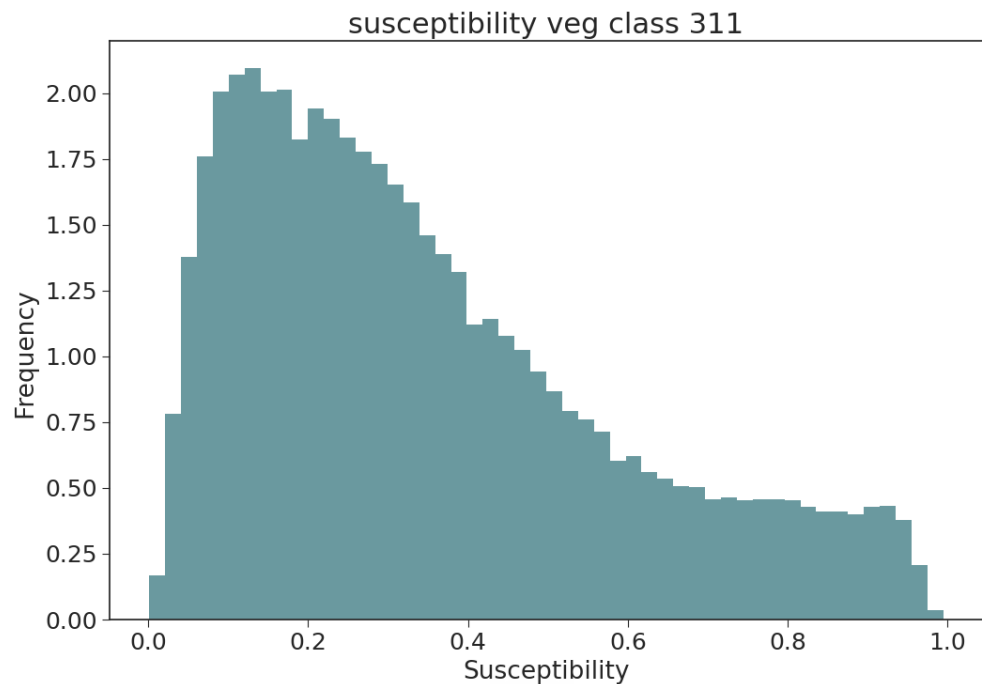


Figure S7. Normalized susceptibility distribution inside the broad leaved in the summer season (class 311).

4. Wildfire susceptibility distribution for Montiferru and Marghine wildfires

In the Results section of the main manuscript, two large fires of 2021 which affected the western part of Sardinia, the Montiferru wildfire (July 2021), and the Marghine fire (August 2021) were presented, see Figure 19. In this Section, the distribution of the susceptibility values given by the summer seasonal map in the two burned areas is presented in detail. In Figure S14, the probability distribution of the pixel spanned by the two wildfires is represented, while Figure S15 portrays the subdivision of the affected pixels into different susceptibility classes.

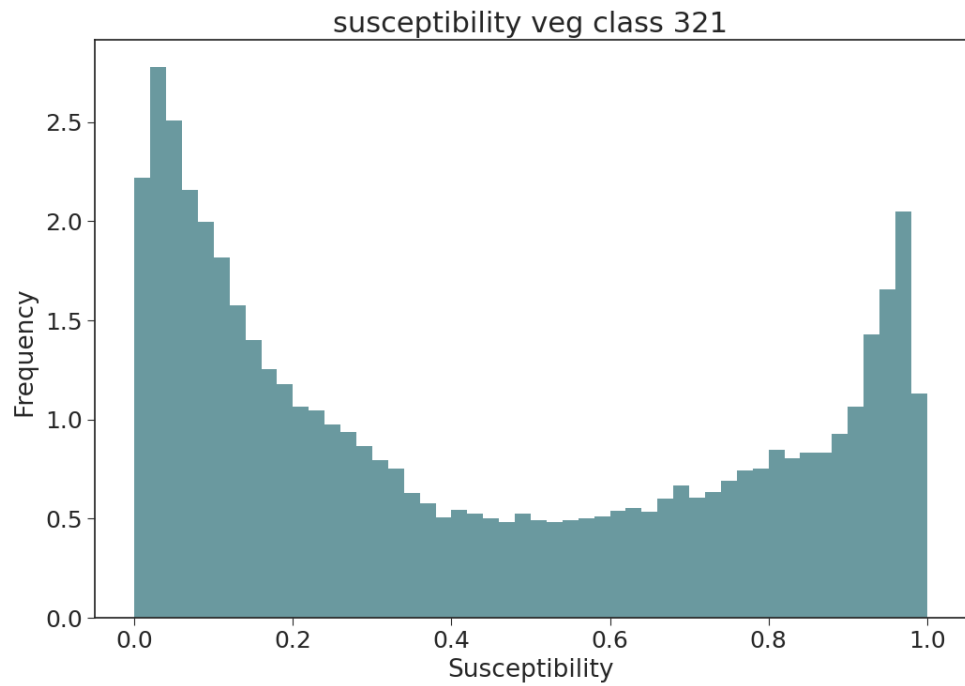


Figure S8. Normalized susceptibility distribution inside the natural grassland in the summer season (class 321).

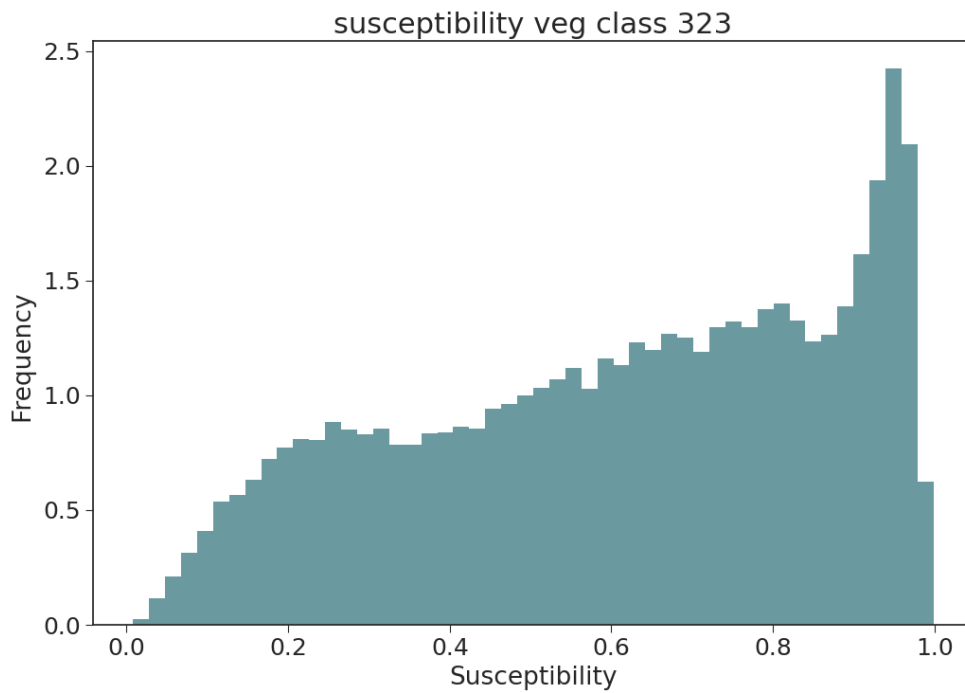


Figure S9. Normalized susceptibility distribution inside the Sclerophyllous vegetation in the summer season (class 323).

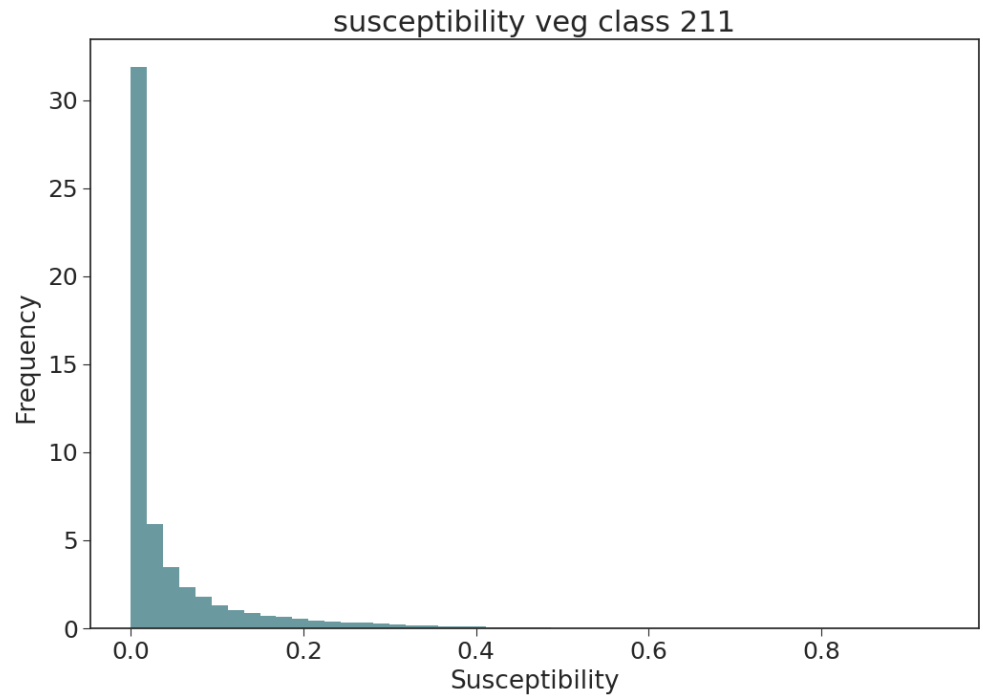


Figure S10. Normalized susceptibility distribution inside the non-irrigated arable land in the winter season (class 211)

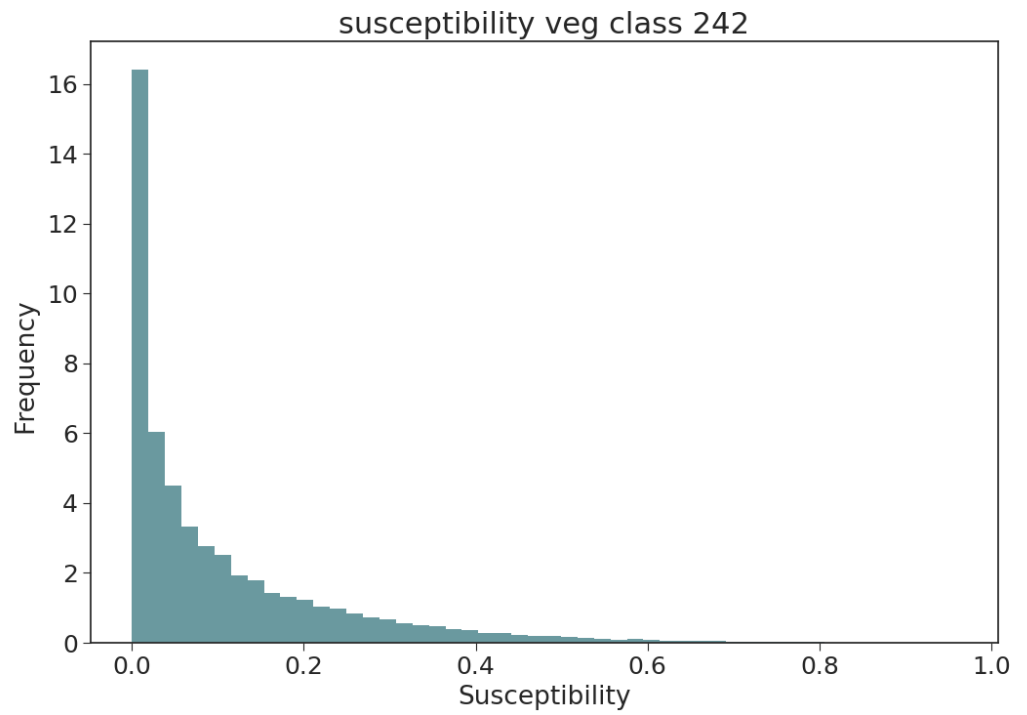


Figure S11. Normalized susceptibility distribution inside the rice fields in the winter season (class 242)

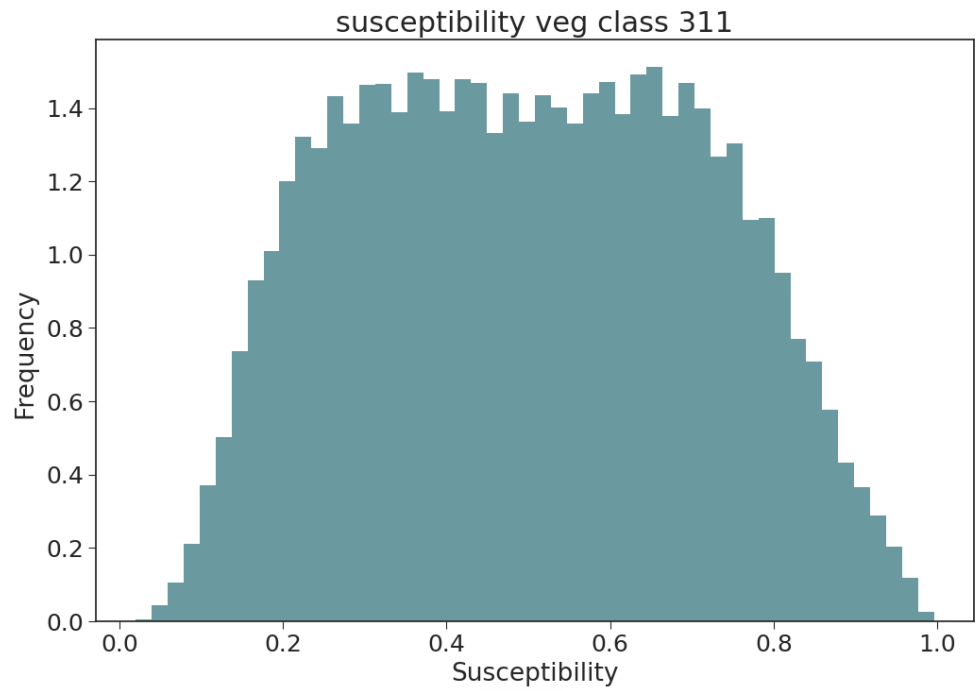


Figure S12. Normalized susceptibility distribution inside the broad leaved in the winter season (class 311)

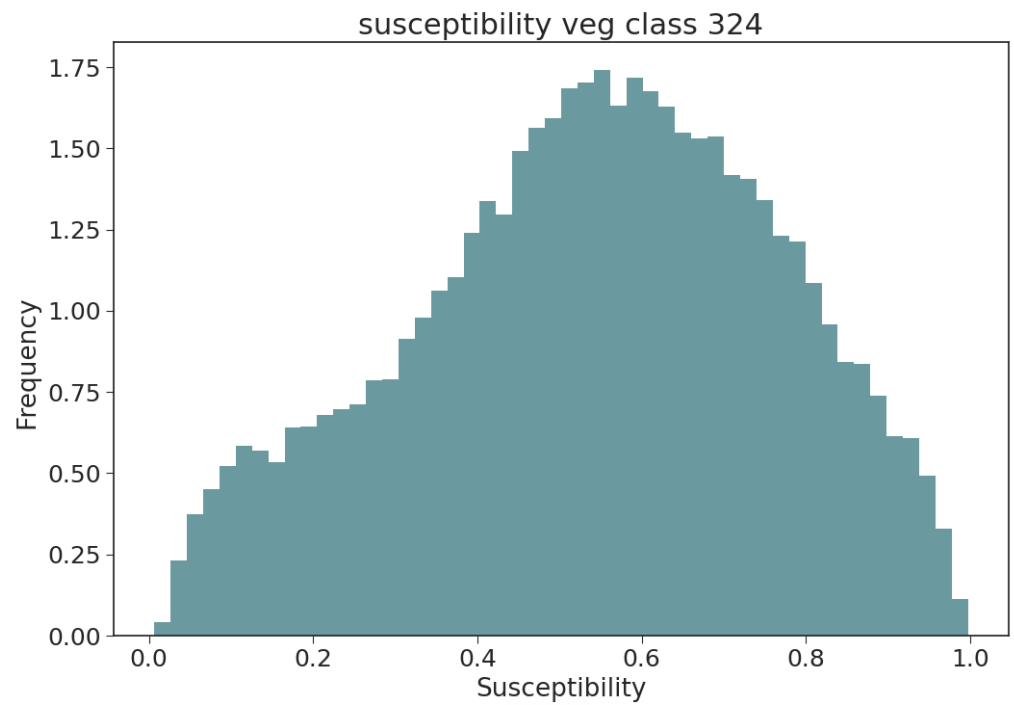


Figure S13. Normalized susceptibility distribution inside the Transitional woodland in the winter season (class 211)

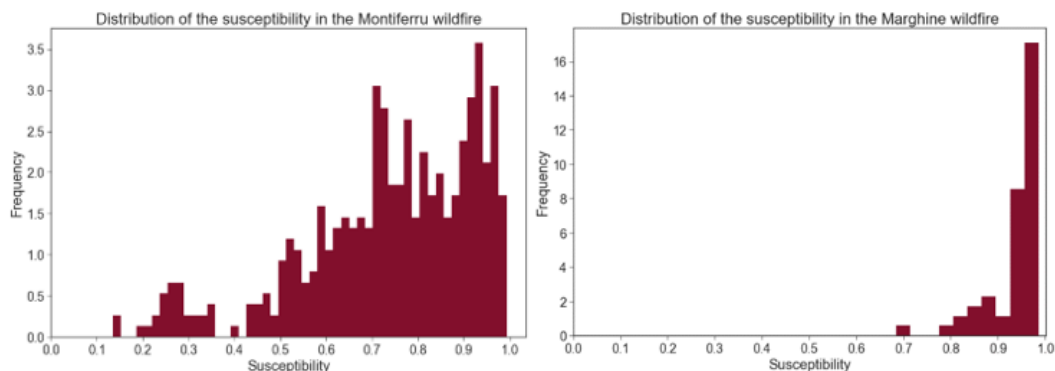


Figure S14. The two histograms refer to the susceptibility distribution in the 2 wildfires presented in Figure 19: the Montiferru wildfire on the left hand side, and the Marghine wildfire on the right hand side. The susceptibility map presents values over 0.5 in almost the totality of the pixel affected by the two wildfires, with a good of values over 0.7.

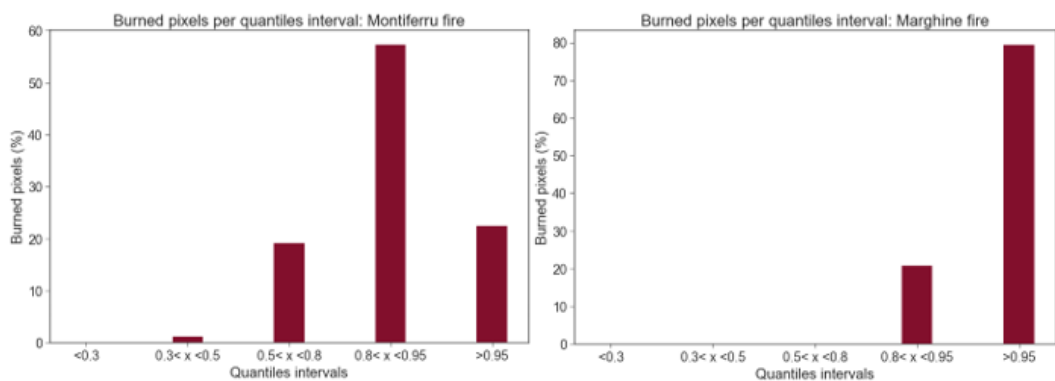


Figure S15. The two histograms refer to the susceptibility distribution in the two considered wildfires. The histogram on the left hand side refers to Montiferru wildfire, while the one on the right hand side to the Marghine wildfire. In both cases, most of the pixels fall on the two highest susceptibility classes.